IOSR Journal of Engineering (IOSRJEN) **www.iosrjen.org**
ISSN (e): 2250-3021, ISSN (p): 2278-8719
Vol. 07, Issue 08 (August. 2017), ||V1|| PP 23-31

Welding Simulation of X70 oil and gas pipeline sheet using various heat sources and experimental validation

Amin Shahinfar*[1], Asghar Habibi Eftekhar[1]
[1]*(Department of Metallurgy, Behbahan Branch, Islamic Azad University, Behbahan, Iran)*
Corresponding author: Amin Shahinfar

Abstract: In this research, Finite Element Modeling (FEM) using SYSWELD was carried out to predict thermal cycles, residual stresses in type X70 oil and gas pipeline sheet weld joint made by TIG welding process. Residual stress were measured using ultrasonic technique (UT) and validated by simulated residual stress profiles. The simulated thermal cycles were validated by thermal cycles measured using thermocouples fitted at 4, 6 and 8 mm from weld line. For modeling, arc voltage, welding current, welding speed, type of thermal source were considered as input parameters and residual stresses and thermal distribution as output parameters. The three heat sources employed were 2D Gaussian, 3D Gaussian and Goldak's double ellipsoid model. There was good agreement between the model predictions and the experimentally observed values of temperature, residual stresses in 2D Gaussian and Goldak heat sources. It was found that the 3D Gaussian heat source predicted the thermal cycles and residual stresses less accurately compared to that of the other heat sources.

Keywords: heat source, residual stresses, Thermal cycle, X70 pipe line, SYSWELD

Date of Submission: 27-07-2017 Date of acceptance: 23-08-2017

I. INTRODUCTION

Fusion welding is a process in which an intense heat source is applied to join components. The material is rapidly heated and it melts to form a weld pool. Once the liquid pool solidifies, two parts are jointed together. The interaction between the base material and the heat source leads to a series of physical and chemical processes which culminate in the final weld composition, geometry, structure and properties. In the solid region around the weld pool, the variation of temperature with time, often referred to as the thermal cycle, may lead to various solid-state phase transformations. [1-3]. Knowledge of the temperature distribution and thermal cycles in the weldment is a prerequisite to understand the development of residual stresses and the extent of the distortions in the weldment [4,5].Prediction of welding thermal cycles and residual stresses using numerical methods through computer simulation has gained popularity in recent years. Among other classical numerical solutions, the finite-element method (FEM) is the most common approach used to model and analyze the welding process. FEM simulation is known as a complementary tool with respect to experimental techniques applied to determine the behavior and interactions between complex physical phenomena in the welding process. Various FEM approaches have been rapidly developed and among most frequently used are thermo-elastic-plastic [8-10], linear thermo-elastic shrinkage [11,12], inherent strain [13,14] and local-global-approach [15]. The main difficulty of the thermal field simulation in a welding process is the heat source modeling. Since Rosenthal (1941) [16] proposed the analytical solution considering a punctual or a line heat source, several more realistic heat source distributions have been developed. Eagar and Tsai (1983) [17], Cho and Kim (2002) [18], Deng et al. [19] and Rayamyaki et al. (2007) [20] developed and applied a surface heat source model based on the Gaussian distribution. Other researchers, such as Balasubramanian et al. (2008) [21], Zaeh and Schober (2008) [22] and Ziolkowski and Brauer (2009) [23], proposed the combination of Gaussian distribution on the surface and distribution along the thickness in order to consider 3D distribution, by applying the conical Gaussian heat source model. Another proposal that uses the same combination, i.e., the Gaussian distribution with the distribution along the thickness, by applying a cylindrical volume along it, was developed by Bachorki et al. (1999) [24]. A classical volumetric heat source model is the double ellipsoid distribution that was developed by Goldak et al. (1984) [25]. Wahab et al. (1998) [26] and Wu et al. (2009) [27] combined the double ellipsoid with spherical and cylindrical volumes along the thickness, respectively.

The surface Gaussian heat source model is generally used for thin plates, where the distribution along the thickness is not important. Therefore, this study investigates its accuracy in welding processes of plates with different thickness. Analyses are performed by the ANSYS® software, considering the convection and the radiation phenomena. Several cases of different parameters of heat distribution, heat input and plate thickness have had their weld pool geometries analyzed and compared with those obtained experimentally. The objective of the present investigation was to identify the proper heat source for accurate predictions of thermal cycles, residual stresses during butt welding of type X70 oil and gas pipeline sheets. Three different heat sources which include 2D Gaussian, 3D Gaussian and Goldak's double ellipsoid model were employed for carrying out the simulation using SYSWELD. The simulated thermal cycles, residual stresses were validated by experimental measurements.

II. EXPERIMENTAL

Shielded metal arc butt welding was carried out in two passes by the manual gas tungsten arc welding process with Direct- Current Electrode Negative on type X70 pipeline sheets of dimensions 300 mm × 200 mm × 4 mm . The specimens were machined to make a 70° V-grooves butt joint with a 2.5 mm root opening gap and a root face of 1 mm. two types of filler materials, ER6010 as root weld and ER7018 as welding filler were employed. The chemical compositions of the base metal are given in Table 1.

Table (1): chemical compositions of the base metal (wt. %)

Base metal	Si	Mn	Cr	Ni	Mo	v	cu	Fe	c
API X70	0.2	1.43	0.15	0.35	0.06	0.055	0.26	ball	0.08

The process parameters employed in the welding include: Peak current: 120 A, voltage: 30 V, welding speed: 2 mm/s, 10 l/min flow rate of argon shielding gas. A specially designed fixture with a copper back plate that could clamp the base metals firmly was employed to avoid distortion and bending while welding. After welding, the weldment were characterized for NDT examination to determine for any flaws, porosities, undercut etc. For metallographic examinations, several specimens were prepared from the transverse cross section of the weldment. The specimens were prepared by grinding using 120, 240, 320,600, 800 and 1200 grits of Sic paper, followed by the final polishing with 5 µm alumina powders. Then, the specimens were etched in Marbel solution (10 g of $CuSO4$+50 cc of HCl+ 50 cc of $H2O$). The microstructural features were investigated using an optical microscope. To test the results of temperature variations during welding and their analogy with simulated samples, R-type thermocouples that can measure temperatures up to 1800 ° C are used. Three thermocouples were fixed respectively at intervals of 4, 6 and 8 mm from the weld line (each thermocouple is 30 mm away from the next thermocouple) as given in Fig. 1. Data from thermocouples at different time intervals are presented in Table 2.

Table (2): Experimental data from thermocouples

	0-20 second	20-40second	40-60 second	60-80second
Thermocouple NO:1	970 ˚C	650˚C	470 ˚C	400˚C
Thermocouple NO:2	880 ˚C	530˚C	400 ˚C	350˚C
Thermocouple NO:2	700 ˚C	450˚C	350 ˚C	-

Longitudinal residual stress profile was measured on the weld joint using an ultrasonic technique described in detail by Palanichamy et al. (2009) [28]. Ultrasonic technique for residual stress measurement is based on the acoustoelastic principle which indicates that propagation velocity of elastic waves depend on the presence of stress in the materials. Accurate ultrasonic transit times were measured in perpendicular to weld direction and across each weld joints. Measured transit times have been converted into quantitative values of residual stresses using the predetermined acoustoelastic constant (AEC) for this steel. The Acoustic Elastic Constant (AEC) for a given material in terms of transit time is given in Eq. (1)

$$B = \frac{t-t_0}{\sigma} \qquad (1)$$

Where t is the measured ultrasonic transit time, t_0 is the transit time measured with zero load condition, σ is the applied or residual stress. The AEC (B) was determined experimentally as 0.605 ns/MPa. The measurements are taken along lines 5 mm apart parallel to the weld line till the farther end of plate. Fig.1 shows the location of the ultrasonic test on the weld piece. Table (3) shows the experimental data from the ultrasonic test.

Table (3): Experimental data from the ultrasonic test (time: nanosecond and stress: MPa)

	1	2	3	4	5	6	7
t	120	250	200	180	300	170	90
t_0	30	30	30	30	30	30	30
σ	148	363	280	247	246	231	99

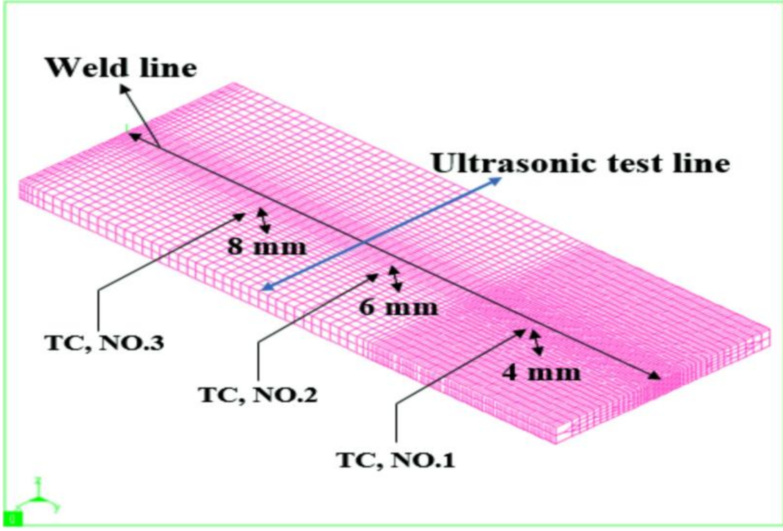

Figure (1): Schematic location of thermocouples (TC) in the path of welding and trajectory of conducting ultrasonic testing.

III. RESULTS AND DISCUSSION

3.1: Analysis of the weld cross section

The results of the software can be shown in various ways, because the program is able to calculate the temperature at any node in the sample under the time scale. In order to assess the ability to predict quantifiable measures in the laboratory, Different models of results require the correct selection of contours. Fig.2 (a, b and c) shows three Contour temperature of heat sources (2D-Gaussian, 3D Gaussian and goldack) in times of 10, 11.33 and 96.5 seconds respectively. The images clearly indicate the high temperature gradient in areas near the thermal source and cold in the remote areas of the welding lines. Fig.2 (C) shows the temperature distribution of the Goldack's thermal source in the weldment. Due to the shape of the temperature distribution in the middle of the weld line, the sample has reached a semi-stable state, which is called quasi-stable state. Away from the heat source, where the heat is greatest. The shape of the molten pool becomes elliptical.

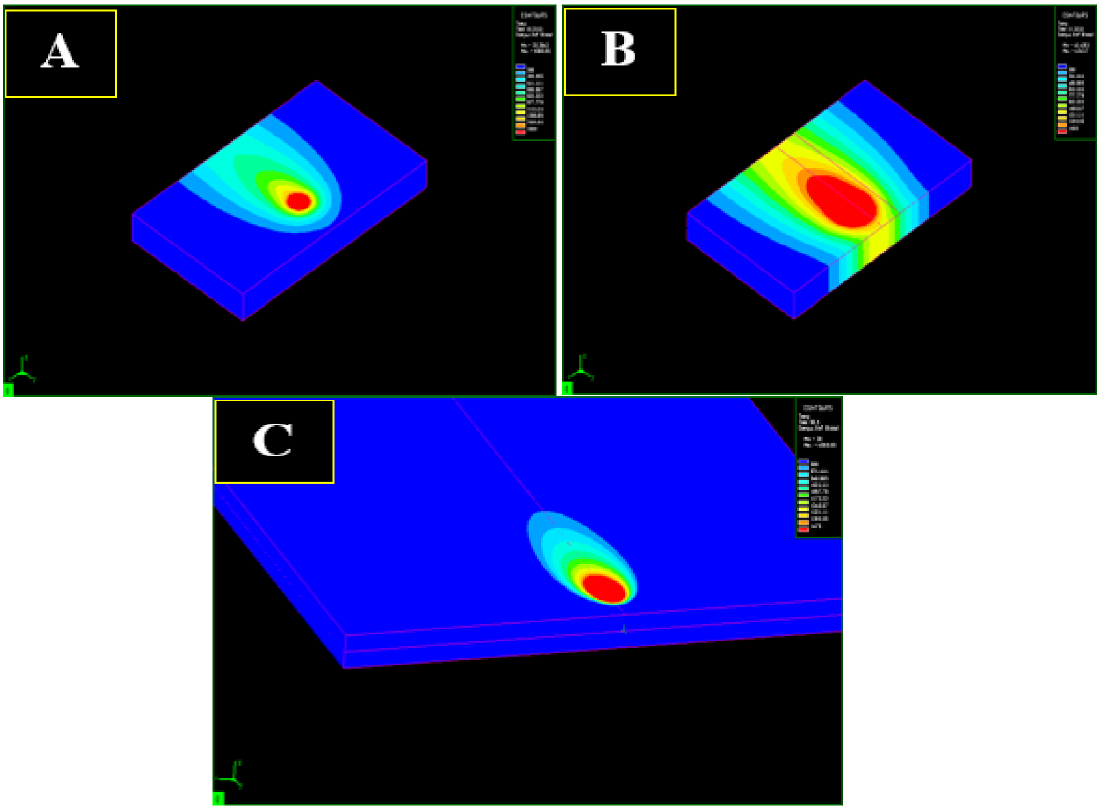

Figure (2): Contour of temperature distribution during the welding process a) two-dimensional Gaussian model, 10 seconds b) three-dimensional Gaussian, time of 11.33 seconds c) Goldak model, time: 96.5 seconds.

Optical microscope image of a cross section of X70 alloy sheets with three cross-sections obtained from simulation models are compared. Fig. 3 (a - d). Fig. 3 (b), (c) and (d) respectively represent the cross section of the simulated 2D Gaussian, 3D cone Gaussian and the Galdak (the two-elliptical model) thermal model.

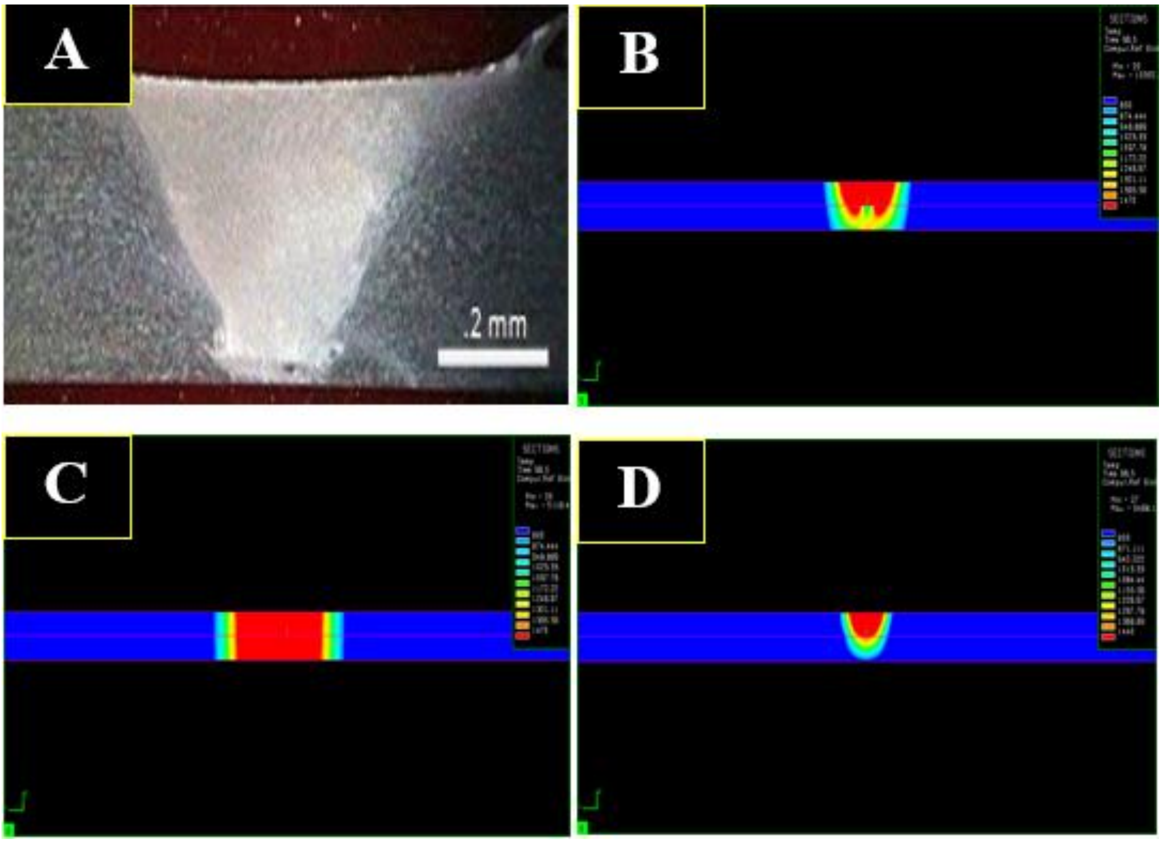

Figure (3): Comparison of cross-sectional area of x70 alloys weldment with simulated samples a) cross-sectional sample of weldment b) contour temperature of two-dimensional Gaussian cross-section c) three-dimensional Gaussian D) model of Goldak

Goldak's heat source compared to other heat sources has more accurate prediction of the cross-sectional area of the weld metal. The 2D-Gaussian model has worked somewhat well at the surface of the welding region, but has not done the proper simulation in the roots of the weld; in general it is difficult to obtain a perfect fit.

3.2: thermal analysis

Fig.4 shows the comparison of thermal analysis simulated by the thermal profile of the software and the experimental data obtained from the laboratory. Fig.4 (a, b, c) shows the comparison of 2D-Gaussian heat profiles with the results of the thermocouples of 1, 2 and 3 respectively.

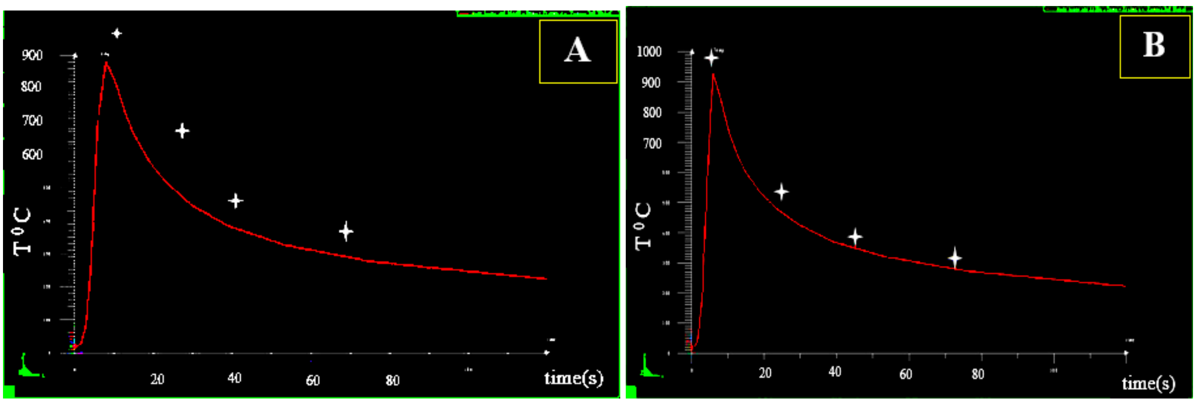

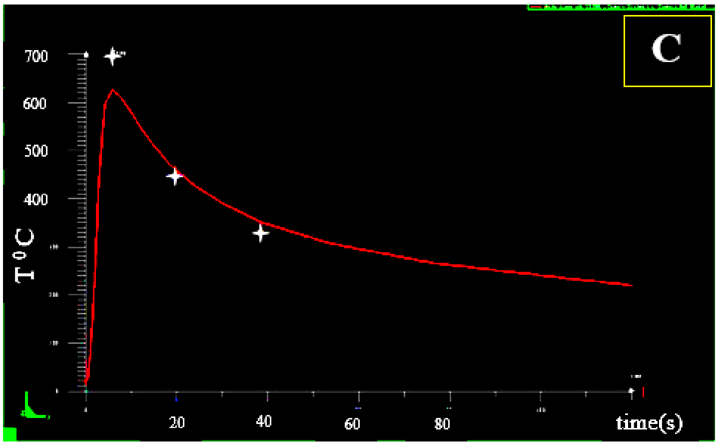

Figure (4): Comparison of experimental and simulated 2D- Gaussian model, solid line represents simulated data and the points representing the experimental data. a) Thermocouple 1 b) Thermocouple 2 and c) thermocouple 3

The maximum temperature in the thermocouples of 1, 2 and 3 is 970 ° C, 880 ° C and 700 ° C, respectively. In the thermocouple number one in the Gaussian 2D-model, the difference in the maximum peak temperature of the simulation and experimental mode is high, but the simulation data of the other two thermocouples is closer to the experimental mode Fig.5 (a, b, c) represents the comparison of the experimental and simulated thermal distribution model of the 3D-Gaussian model in thermocouples No. 1, 2 and 3.

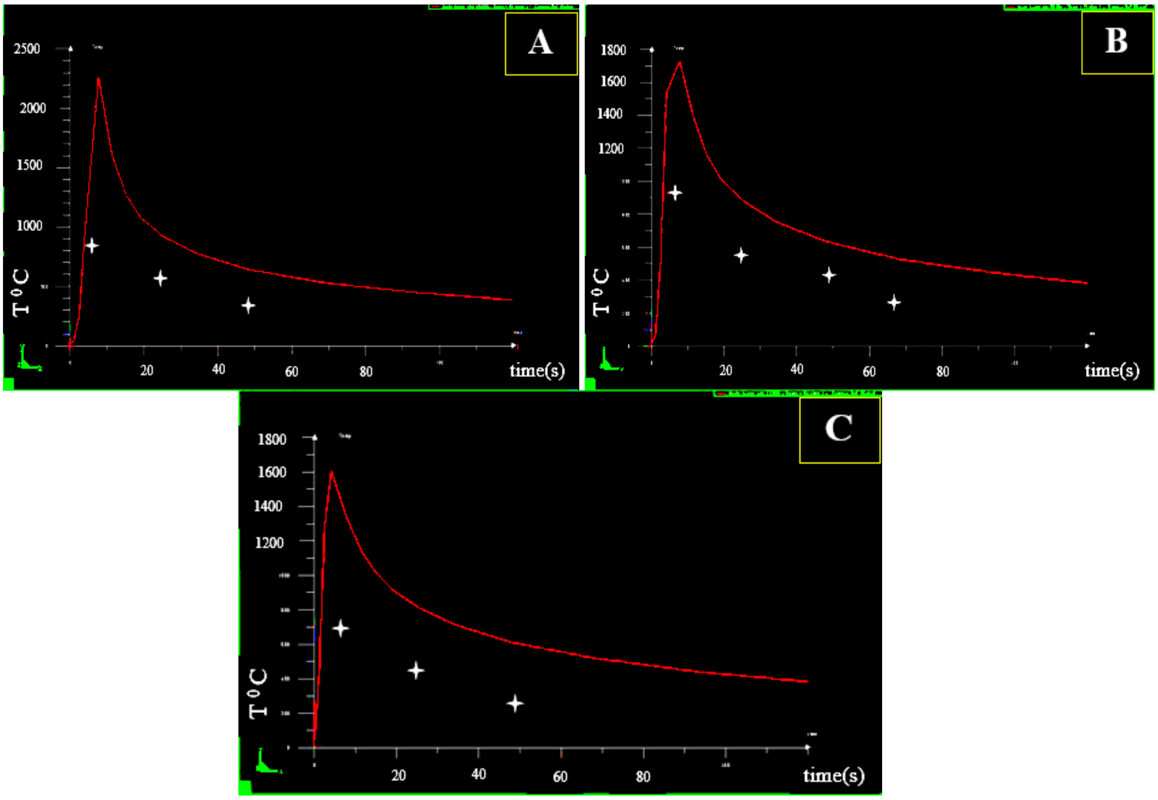

Figure (5): Comparison of experimental and simulated 3D- Gaussian model, solid line represents simulated data and the points representing the experimental data. a) Thermocouple 1 b) Thermocouple 2 and c) thermocouple 3

The maximum thermal peak in thermocouple number 1 is obtained by the software at approximately 2300 ° C, which has a significant difference with the experimental value (880 ° C). Measured values at other intervals also have significant differences with experimental values. At Fig.5 (B), the 3D-Gaussian thermal model represents a maximum temperature of 1720 ° c for thermocouples (2), while this value is 880 ° C for the laboratory mode, however, in other cases there are significant differences. The 3D-Gaussian model for the thermocouple (3) according to Fig.5(C) shows a difference of approximately 750 ° C for the simulated model and experimental data, which shows that this thermal model cannot be used to predict the heat distribution of the weld. Fig.6 (a, b and c) represents the comparison of simulated Goldak model and experimental data.

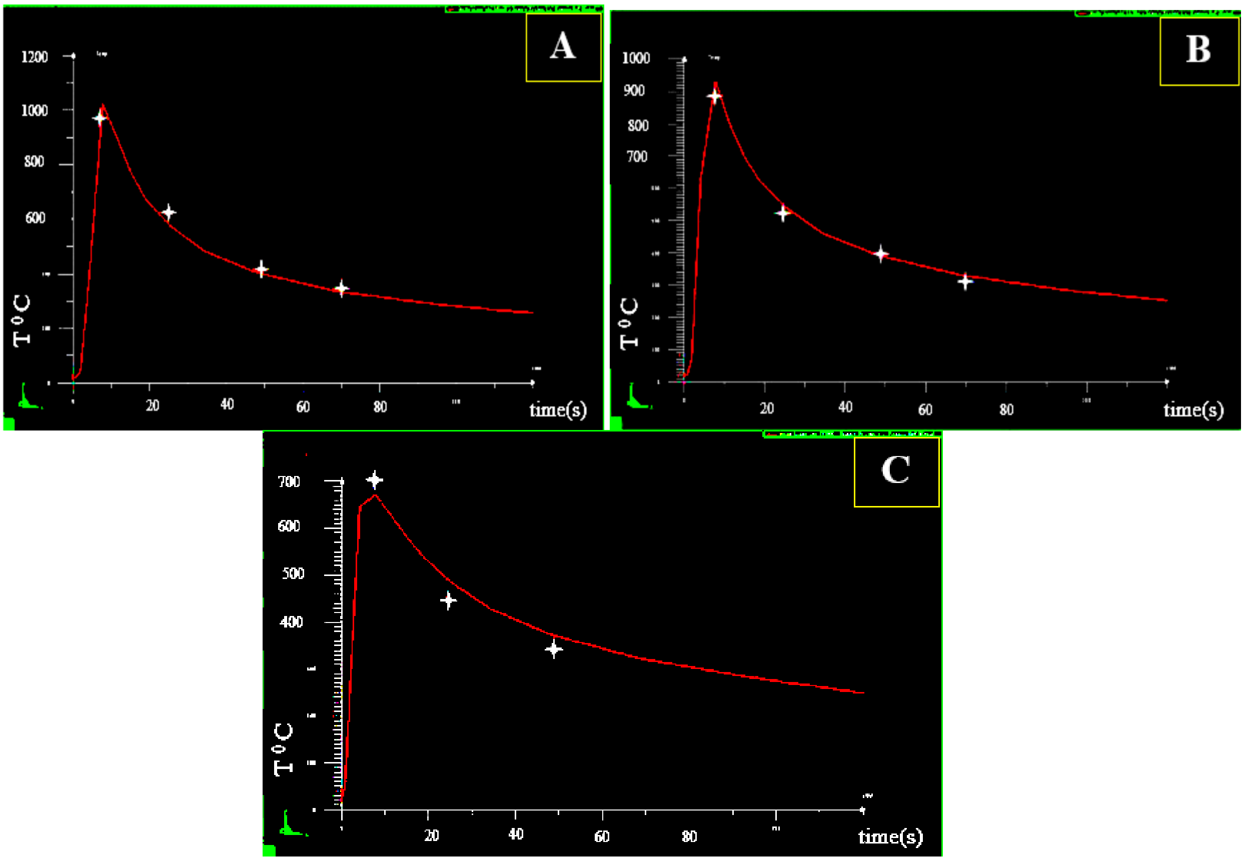

Figure (6): Comparison of experimental and simulated goldack model, solid line represents simulated data and the points representing the experimental data. A) Thermocouple 1 B) Thermocouple 2 and C) thermocouple 3

The thermal peak in the first thermocouple is 970 ° C, which has little difference with the temperature peak of Fig. 4-5 (a), which is about 1050 ° C, and the rest of the experimental data have very little difference with the simulated data. The small difference between experimental and numerical data in Figures 4-5 (A, B, and C) shows that the Goldak's model is the best thermal source for simulating this type of welding, This can be due to the constants used in the model and the increase of thermal conductivity with regards to the thermal conduction transfer [29]. For 2D-Gaussian and Goldak's models, the difference in data is below 100 ° C, which can be an acceptable range. Overall, two-dimensional Gaussian corresponds to some extent, the three-dimensional cone does not fit much. Goldak's model (two cones) has the best thermal compatibility.

3.3: residual stress

Fig.7 (a, b and c) represents the data obtained from the simulation of the residual stress under three thermal sources with the data obtained from the ultrasonic test.

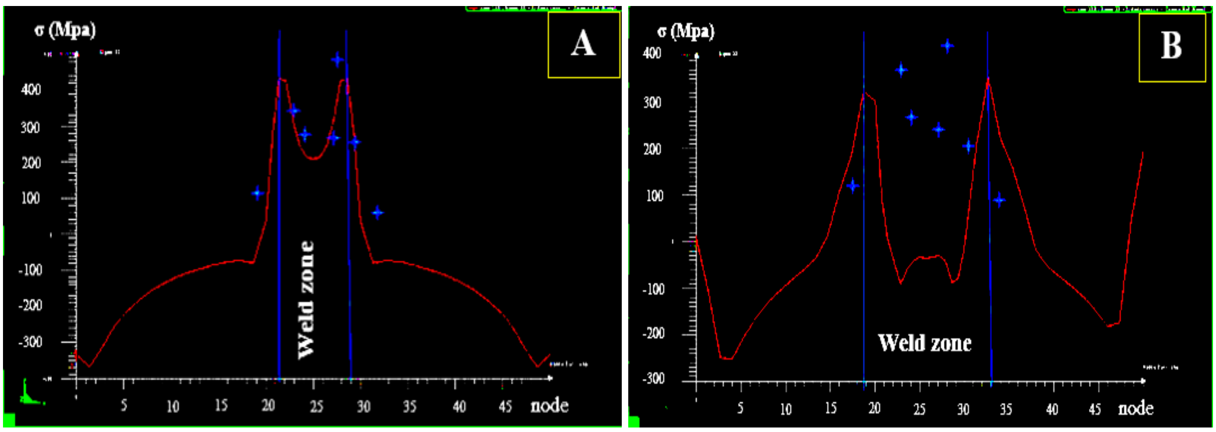

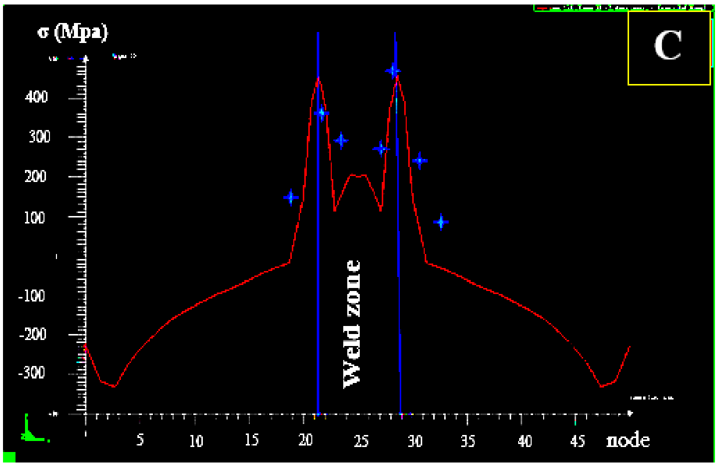

Figure (7): Comparison of data from residual stresses by software and ultrasonic testing, solid lines and simulated data and points represent simulated data and experimental data respectively. A) Residual stress in 2D-Gaussian B) 3D- Gaussian C) Goldak mode.

The residual stress along the line perpendicular to the weld cross section is approximately the same for the 2D- Gaussian and Goldak's models, but these data are very different in the 3D-Gaussian model. The high residual tensile stress in some places is due to the balance between freezing in the weld bed and the resistance to the base metal shrinkage, which occurs more often near the weld line. At distances farther from the weld line, the compressive stress is higher. The maximum tensile residual stress in the two-dimensional Gaussian model, Gaussian and Goldak's model are 434, 355, and 458 MPa, respectively. While the maximum tensile stress obtained in the experimental test is 468 MPa. Profile obtained with two models of two-dimensional Gaussian heat source and Goldak's model are almost identical. In these two models, the data is matched fairly well together. Differences in the data could also be due to experimental error and simulation solutions. Fig.8 (a, b) represent the simulated macrograph of the residual stress after welding in the two-dimensional Gaussian model and the Goldak model. As shown in Fig.8, by moving away from the weld line, tensile stress changes to the compression stress and we have the compressive residual stress at the edge of the workpiece.

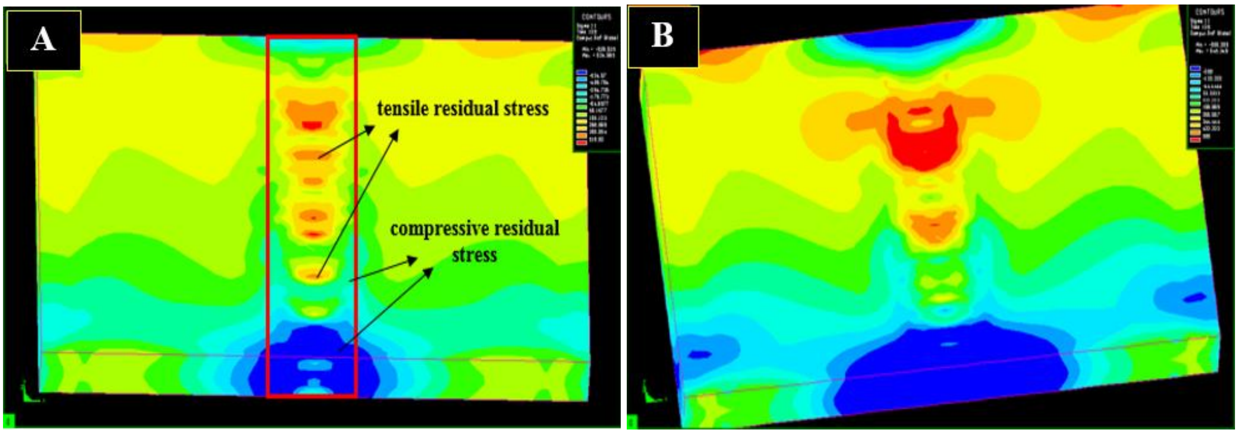

Figure (8): residual stress macrograph A) 2D- Gaussian model B) Goldak model

IV. CONCLUSION

1. Two-dimensional Gaussian heat sources and Goldak model provide correct prediction with maximum values obtained from thermocouples and their differences are low.
2. Goldak thermal model has better prediction of welding cross section than 2D-Gaussian thermal model.
3. The data obtained from the ultrasonic test are in good agreement with the data obtained from Goldak and two-dimensional Gaussian heat models.
4. The maximum tensile stress at the weld bead and there is more compressive stress in the base metal.
5- 3D- Gaussian thermal model does not provide an accurate prediction of the heat distribution and residual stress in the weld area.

REFERENCES

[1] T. DebRoy and S. Kou: Heat Flow in Welding, Chapter 3, Welding Handbook, vol. 1, 9th Edition, American Welding Society, 2001, pp. 87-113.

[2] J. F. Lancaster: The Physics of Welding 2nd Edition, Pergamon, Oxford, 1986.

[3] K. Easterling: Introduction to the Physical Metallurgy of Welding, 2nd Edition, Butterworth-Heinemann, Oxford, 1992.

[4] Ø. Grong: Metallurgical Modeling of Welding, 2nd edition, The Institute of Materials, London, 1997

[5] S. Kou: Welding Metallurgy, 2nd edition, John Wiley & Sons, Hoboken, New Jersey, 2003.

[6] Bang Han-Sur, Kim Young-Pyo, Joo Subg-Min, Kim Jong-Myung, Hwang Won-Sup. A study on the mechanical behaviours in welded parts by numerical simulation. Key Engineering Materials 2004; 270-273:2371-6.

[7] Kim Juwan, Im Seyoung, Kim Hyun-Gyu. Numerical implementation of thermoelasticplastic constitutive equation in consideration of transformation plasticity in welding. International Journal of Plasticity 2005; 21:1383-408.

[8] Bang Han-Sur, Kim Young-Pyo, Joo Subg-Min, Kim Jong-Myung, Hwang Won-Sup. A study on the mechanical behaviours in welded parts by numerical simulation. Key Engineering Materials 2004; 270-273:2371-6.

[9] Kim Juwan, Im Seyoung, Kim Hyun-Gyu. Numerical implementation of thermoelasticplastic constituitive equation in consideration of transformation plasticity in welding. International Journal of Plasticity 2005; 21:1383-408.

[10] Mollicone P, Camilleri D, Gray TGF, Comlekci T. Simple thermo-elastic-plastic models for welding distortion simulation. Journal of Materials Processing Technology 2006; 176:77-86.

[11] Slovacek Marek, Kovarik Jiri, Tejc Josef. Using of welding virtual numerical simulation as the technical support for industrial. In: The 5th international scientific-professional conference SBW 2009 robotization and automation in welding and other techniques, Slavonski Brod 2009. p. 75-82.

[12] Lu Yao-hui, Wu Ping-bo, Zeng Jing, Wu Xing-wen. Numerical simulation of welding distortion using shrinkage force approach and application. Advanced Materials Research 2010; 129-131:867-71.

[13] Li Hong, Ren Huilong. Prediction of welding distortions of stainless steel ship.Key Engineering Materials 2007; 284-349:373-6.

[14] Wang YX, Zhang P, Hou ZG, Li CZ. Inherent strain method and thermal elasticplastic analysis of welding deformation of a thin-wall beam. Journal of MechanicsDecember 2008; 24(4):301-9.

[15] Souloumiac B, Boitout F, Bergheau JM. A new local-global approach for the modelling of welded steel component distortions. Mathematical Modelling of Weld Phenomena 2002; 6:573-90.

[16] Rosenthal, D., 1941. "Mathematical theory of heat distribution during welding and cutting". Welding Journal, Vol. 20 (5), p. 220s-234s.

[17] Eagar, T.W. and Tsai, N.S., 1983. "Temperature fields produced by traveling distributed heat sources". Welding Journal, Vol. 62 (12), p. 346-355.

[18] Cho, S.H. and Kim, J.W., 2002. "Analysis of residual stress in carbon steel weldment incorporating phase transformations". Science and Technology of Welding and Joining, Vol. 7 (4), p. 212-216.

[19] Deng, D. and Murakawa, H., 2008. "Prediction of welding distortion and residual stress in a thin plate butt-welded joint". Computational Materials Science, Vol. 43, p. 353-365.

[20] Rayamyaki, P., Karkhin, V.A. and Khomich, P.N., 2007. "Determination of the main characteristics of the temperature field for the evaluation of the type of solidification of weld metal in fusion welding". Welding International, Vol. 8, p. 600-604.

[21] Balasubramanian, K.R., Siva Shanmugam, N., Buvanashekaran, G. and Sankaranayanasamy, K., 2008. "Numerical and experimental investigation of laser beam welding of AISI304 stainless steel sheet". Advances in Production Engineering & Management, Vol. 3 (2), p. 93-105.

[22] Zaeh, M.F. and Schober, A., 2008. "Approach for modelling process effects during friction stir welding of composite extruded profiles". Advanced Materials Research, Vol. 43, p. 105-110

[23] Ziolkowski, M. and Brauer, H., 2009. Modeling of Seebeck effect in eletron beam deeep welding of dissimilar metals. The International Journal for Computation and Mathematic in Electric and Electronic Engineering, v. 28, p. 140-153.

[24] Bachorki, A., Painter, M. J., Smailes, A.J. and Wahab, M.A., 1999. "Finite-element prediction of distortion during gas metal arc welding using the shrinkage volume approach". Journal of Materials Processing Technology, Vol. 92-93, p. 405-409.

[25] Goldak, J.A., Chakravarti, A., Bibby, M., 1984. "A new finite element model for welding heat sources". Metallurgical Transactions, Vol. 15, p. 299-305.

[26] Wahab, M.A., Painter, M.J. and Davies, M.H., 1998. "The prediction of the temperature distribution and weld pool geometry in the gas metal arc welding process". Journal of Materials Processing Technology, Vol. 77, p. 233-239.

[27] Wu, C.S., Hu, Q.X., Gao, J.Q., 2009. "An adaptive heat source model for finite-element analysis of key hole plasma arc welding". Computational Material Science, Vol. 46, p. 167-172.

[28] Palanichamy, P., Vasudevan, M., Jayakumar, T., 2009. Measurement of residual stresses in austenitic stainless steel weld joints using ultrasonic techniques. Sci. Technol. Weld. Join. 14, 166–171.

[29] Simulation of laser butt welding of AISI 316L stainless steel sheetusing various heat sources and experimental validation; Jazeel Rahman Chukkan, M. Vasudevan,; Journal of Materials Processing Technology 219 (2015) 48–59.

Amin Shahinfar. "Welding Simulation of X70 oil and gas pipeline sheet using various heat sources and experimental validation ." IOSR Journal of Engineering (IOSRJEN), vol. 7, no. 8, 2017, pp. 23–31.